Simulation of solitons in an Ising-like $S=\frac{1}{2}$ antiferromagnet on a linear chain

F. Matsubara and S. Inawashiro
Department of Applied Physics, Tohoku University, Sendai 980, Japan
(Received 31 July 1989)

The dynamics of quantum solitons in an Ising-like $S=\frac{1}{2}$ antiferromagnet on finite linear chains with spins $N(\leq 15)$ is studied by integrating the Schrödinger equation of motion. Space-time correlation functions $S^{zz}(r,t)$ and their Fourier transforms, i.e., dynamical structure factor $S^{zz}(q,\omega)$, are calculated for both even and odd N. A slow but large oscillation of $S^{zz}(r,t)$ is seen, which gives a direct evidence of the occurrence of propagating domain walls, i.e., solitons. The oscillation leads to a low-energy component of $S^{zz}(q,\omega)$ whose line shape greatly depends on whether N is even or odd and on the temperature. We analyze in detail the dependence of soliton number in the line shape and give a plausible conjecture that $S^{zz}(q,\omega)$ for $N=\infty$ should exhibit a very broad double maximum at low temperatures. We estimate $S^{zz}(q,\omega)$ at various temperatures. Our results reproduce experimental observations of $S^{zz}(q,\omega)$ on $CsCoCl_3$ and $CsCoBr_3$ very well over a wide temperature range.

I. INTRODUCTION

Propagating domain walls or solitons in a one-dimensional (1D) magnetic system have been a subject of great interest in the past decade. For example, the Hamiltonian of classical planar spins on a 1D chain in a magnetic field can be reduced to a sine-Gordon Hamiltonian in which a well-known broad soliton solution exists.[1,2] Ferromagnetic compound $CsNiFe_3$ (Ref. 3) and antiferromagnetic compounds $(CH_3)_4NMnCl_3$ (Ref. 4) are known realizations of the model. Many experiments have shown evidence of the occurrence of solitons in the compounds, and now there is no doubt that solitons really occur.[5] However, low-lying excitations in the compounds are magnons and the contribution of solitons to magnetic quantities are difficult to know quantitatively because of interferences between magnons and solitons.[6,7] On the other hand, in an $S=\frac{1}{2}$ antiferromagnetic Ising-like model, low-lying excitations are solitons characterized by propagating distinct domain walls, and their contribution to magnetic quantities can readily be investigated. Villain first gave the soliton picture and predicted that solitons lead to a low-energy component of the longitudinal neutron scattering, $S^{zz}(q,\omega)$.[8] The compounds $CsCoCl_3$ and $CsCoBr_3$ are known to be good realizations of the Ising-like model, and solitons in these compounds have been extensively studied using various experimental techniques such as Raman scattering,[9] NMR,[10] ESR,[11,12] and neutron scattering.[13–17] However, there remains a strong discrepancy between Villain's prediction on the scattering function $S^{zz}(q,\omega)$ and experimental observations. Square-root singularities are predicted to occur at cutoff energies $\pm\Omega(q)$, whereas experimental observations reveal the occurrence of a very broad maximum or shoulder around $\Omega(q)$.[13,15,16] The discrepancy has been said to occur because of neglect of the interactions of solitons, and several attempts have been made to take into account the interactions.[15,16] Comparisons between the theoretical and experimental results, however, have remained unsatisfactory. Exact calculation of $S^{zz}(q,\omega)$ of a finite chain with the spin number up to $N=10$ was also made.[18] It clearly revealed the occurrence of the soliton mode peak, but, because of the smallness of the system, it did not predict the line shape of $S^{zz}(q,\omega)$ in a larger system.

Our question is whether the purely 1D Ising-like model reproduces the experimental structure factor $S^{zz}(q,\omega)$ or whether any other mechanism is necessary in order to explain the experimental results. To answer this question, we need to make an accurate calculation of the interactions of solitons and/or to make an exact calculation of $S^{zz}(q,\omega)$ in a larger system. In this paper, we propose a quantum Monte Carlo method of studying the dynamics of a larger system. Our method is based on a numerical integration of the Schrödinger equation of motion. To obtain the thermal averages of quantities of interest, a Monte Carlo method of random sampling of states is also used.[19,20] Correlation functions of two spins $S^{zz}(r,t)$ are calculated and the structure factors $S^{zz}(q,\omega)$ are obtained in terms of Fourier transforms of the correlation functions. We calculate $S^{zz}(q,\omega)$ for different N at different temperatures and show that the line shape depends on whether N is even or odd and on the temperature. We argue in detail about the mechanism responsible for the line shape of $S^{zz}(q,\omega)$ and give a plausible prediction about the line shape for a larger N. To support the argument, we also calculate $S^{zz}(q,\omega)$ of the model in a subspace consisting of low-lying Ising states by using a conventional diagonalization technique. Using the results, we make an extrapolation of $S^{zz}(q,\omega)$ to a larger N. Our results are compared with experimental results on $CsCoCl_3$ and $CsCoBr_3$.

The model and the soliton picture are briefly reviewed in Sec. II. A quantum Monte Carlo method is explained in Sec. III. In Sec. IV, the structure factor $S^{zz}(q,\omega)$ is obtained using the method, and its properties are discussed in detail. In Sec. V, $S^{zz}(q,\omega)$ is calculated by the diago-

nalization technique, and the contribution of individual soliton states to $S^{zz}(q,\omega)$ is analyzed. In Sec. VI, comparisons between our results and experimental observations are made. Section VII is devoted to conclusions.

II. MODEL AND SOLITON PICTURE

We start with the model of N spins on a linear chain described by

$$H=2J\sum_i [S_i^z S_{i+1}^z+\epsilon(S_i^x S_{i+1}^x+S_i^y S_{i+1}^y)] , \quad (2.1)$$

where $S=\frac{1}{2}$, $\epsilon \ll 1$, and the periodic boundary condition is assumed. Before giving the results of our analyses, we briefly review the soliton picture of the model and a resulting structure factor $S^{zz}(q,\omega)$. Since $\epsilon \ll 1$, the ground state of the model is close to the doubly degenerate Néel states. This is realized when N is even because of the boundary condition. For odd N, the lowest energy states are ones in which a single localized domain wall exists. This domain wall exhibits a propagating behavior[8] and is called a soliton. A single soliton characterized by a wave vector q has energy

$$\omega=J[1+2\epsilon\cos(2q)]$$

and moves with velocity $v=4\epsilon J\sin(2q)$, where $0\le q<\pi$. A resulting structure factor $S^{zz}(q,\omega)$ exhibits a square-root singularity at cutoff energies

$$\pm\Omega(q)\ [=4\epsilon J|\sin(q)|] .$$

Low-lying states described by solitons for odd and even N are schematically illustrated in Fig. 1.

For even N, low-lying excitations are described by a domain-wall pair (two solitons). Ishimura and Shiba[18] solved the problem and showed that the excitation spectrum of two solitons is given by

$$\omega=2J[1+2\epsilon\cos(q)\cos(q+\phi)]$$

with $-\pi<\phi<\pi$. Using the solution, Nagler *et al.*[15] showed that two-soliton states also lead to the same square-root singularity of $S^{zz}(q,\omega)$. From the results, they conjectured that any calculation in which the number of domain walls is conserved should yield essentially the same line shape of $S^{zz}(q,\omega)$.

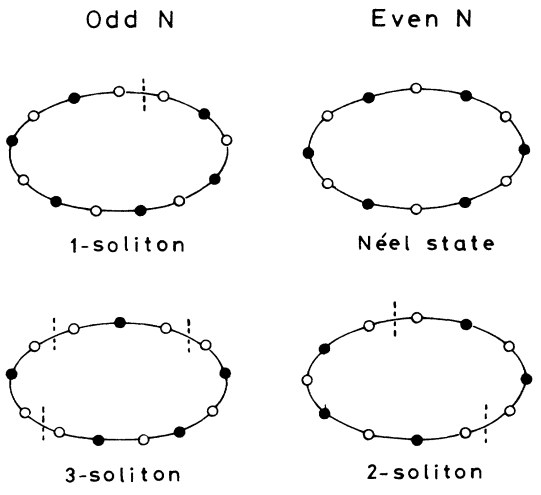

FIG. 1. Schematic illustrations of soliton states for odd and even N. Open and solid circles indicate up and down spins, respectively.

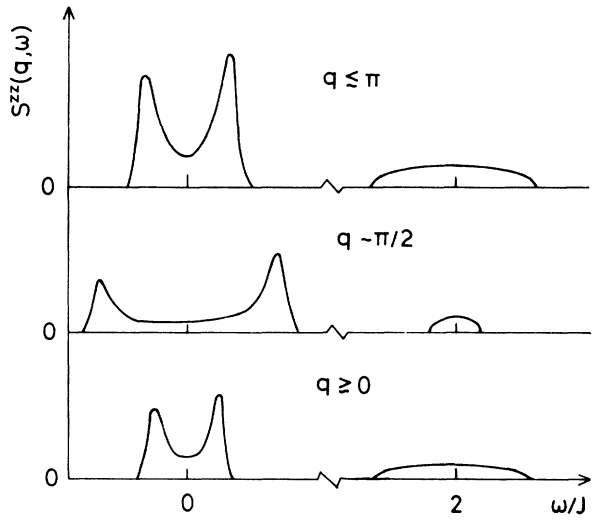

FIG. 2. Schematic line shapes of $S^{zz}(q,\omega)$ obtained using the soliton picture of the 1D Ising-like model.

At finite temperatures, many solitons are thermally excited, and interactions between them occur. Villain[8] qualitatively discussed this problem and suggested that the square-root singularity will be broadened due to collisions between solitons. A quantitative treatment of the collisions was made by Boucher *et al.*,[16] and, in fact, a rounded off double peak is obtained at just below $\Omega(q)$. The line shapes of $S^{zz}(q,\omega)$ obtained so far are schematically illustrated in Fig. 2, for which experimental resolutions are also taken into account.[15,16] We note that, as pointed out in Sec. I, the line shapes differ from those observed in the experiments on $CsCoBr_3$ (Ref. 15) and $CsCoCl_3$ (Refs. 13 and 16). The theoretical ones shown in Fig. 2 have distinct humplike peaks, whereas those observed in experiments exhibit much broader peaks or shoulders as will be cited in Sec. VI.

III. MONTE CARLO METHOD FOR QUANTUM DYNAMICS

We consider pair-correlation functions of spins

$$S^{\eta\eta}(r,t)\ [=\langle S_i^{\eta}(0)S_{i+r}^{\eta}(t)\rangle]$$

defined by

$$S^{\eta\eta}(r,t)=\sum_{\alpha=1}^{2^N}\langle\alpha|S_i^{\eta}e^{iHt}S_{i+r}^{\eta}e^{-iHt}e^{-\beta H}|\alpha\rangle\Big/\sum_{\alpha=1}^{2^N}\langle\alpha|e^{-\beta H}|\alpha\rangle\ , \tag{3.1}$$

where $\beta=1/T$. Here t and T are time and temperature measured in the units of $\hbar=1$ and $k_B=1$, respectively. $\{|\alpha\rangle\}$ is an arbitrary complete orthonormal set. Here we choose $|\alpha\rangle$ as Ising states. The correlation functions are approximately calculated using a Monte Carlo method of random sampling of states.[19,20] That is

$$\begin{aligned}S^{\eta\eta}(r,t)&=\sum_{k=1}^{M}\langle\psi_k|S_i^{\eta}e^{iHt}S_{i+r}^{\eta}e^{-iHt}e^{-\beta H}|\psi_k\rangle\Big/\sum_{k=1}^{M}\langle\psi_k|e^{-\beta H}|\psi_k\rangle\\&=\sum_{k=1}^{M}\langle\bar{\psi}_k|S_i^{\eta}e^{iHt}S_{i+r}^{\eta}e^{-iHt}|\bar{\psi}_k\rangle\Big/\sum_{k=1}^{M}\langle\bar{\psi}_k|\bar{\psi}_k\rangle\ ,\end{aligned} \tag{3.2}$$

where $|\psi_k\rangle$ is defined as

$$|\psi_k\rangle=\sum_{\alpha=1}^{2^N}C_{\alpha}^{k}|\alpha\rangle\ , \tag{3.3}$$

and $|\bar{\psi}_k\rangle=e^{-\beta H/2}|\psi_k\rangle$. Here C_{α}^{k} is a random number for $-1<C_{\alpha}^{k}<1$. Numerical errors in obtaining the correlation functions by using Eq. (3.2) instead of Eq. (3.1) are estimated to be of order $1/\sqrt{M}$; since C_{α}^{k} is a random number then

$$\frac{3}{M}\sum_{k=1}^{M}C_{\alpha}^{k}C_{\alpha'}^{k}\rightarrow\delta_{\alpha,\alpha'}+O(1/\sqrt{M})\ , \tag{3.4}$$

holds for $M\rightarrow\infty$.

Equation (3.2) is calculated by the following procedure. (1) We first give a state $|\psi_k\rangle$ according to Eq. (3.3), which is one at $T=\infty$, then operate $\exp(-\beta H/2)$ to the state yielding a state at a temperature $2T$. (2) Wave functions $|\bar{\psi}_k\rangle$ and $\langle\bar{\psi}_k|S_i^{\eta}$ at $t=0,\tau,2\tau,\ldots$, for $J\tau\ll1$, which are denoted as $|\bar{\psi}_k(n)\rangle$ and $\langle\bar{\psi}_k S_i^{\eta}(n)|$ hereafter, can successively be calculated by operating $\exp(-iH\tau)$ to the functions. In this calculation, since the model considered here is Ising like and the wave functions are expressed in terms of Ising states, one can use the following expansion of $e^{-iH\tau}$:

$$e^{-iH\tau}=e^{-iH_z\tau}\left[1-\int_0^{i\tau}dt\,e^{H_z t}H_{xy}e^{-H_z t}+\int_0^{i\tau}dt\int_0^{t}dt'e^{H_z t}H_{xy}e^{-H_z t}e^{H_z t'}H_{xy}e^{-H_z t'}+\cdots\right]\ , \tag{3.5}$$

with

$$H_z=2J\sum_{i=1}S_i^zS_{i+1}^z,\quad H_{xy}=2J\epsilon\sum_{i=1}(S_i^xS_{i+1}^x+S_i^yS_{i+1}^y)\ , \tag{3.6}$$

Time evolution of each Ising state $|\alpha\rangle$ is then described as

$$\begin{aligned}e^{-iH\tau}|\alpha\rangle=&e^{-iE_{\alpha}\tau}|\alpha\rangle+\sum_{\alpha'}\frac{e^{-iE_{\alpha'}\tau}-e^{-iE_{\alpha}\tau}}{E_{\alpha'}-E_{\alpha}}W_{\alpha'\alpha}|\alpha'\rangle\\&-\tfrac{1}{2}\tau^2\sum_{\alpha'}\sum_{\alpha''}e^{-iE_{\alpha''}\tau}W_{\alpha''\alpha'}W_{\alpha'\alpha}|\alpha''\rangle\ ,\end{aligned} \tag{3.7}$$

where $H_z|\alpha\rangle=E_{\alpha}|\alpha\rangle$ and $W_{\alpha\alpha'}=\langle\alpha|H_{xy}|\alpha'\rangle$ and, in the third term of the right-hand side, only the lowest power in $J\tau$ is taken into account for simplicity. This method can also be used to obtain $|\bar{\psi}_k\rangle$. In the course of calculating the time evolution of the wave functions, numerical errors also occur. These can roughly be estimated by calculating conserved quantities such as the energy of the system and the norms of the wave functions. To avoid compounding the errors, we renormalize the wave functions for every step and calculate the energy to check the accuracy of the approximation. Typically, when $\epsilon=0.1$ and $J\tau=\frac{1}{4}$, the relative difference in the energy is less than 0.5% for $Jt=400$.

The correlation functions $S^{\eta\eta}(r,t)$ for discrete times $t=nJ\tau$ are calculated by

$$S^{\eta\eta}(r,t)=\sum_{k=1}^{M}\langle\bar{\psi}_k S_i^{\eta}(\eta)|S_{i+r}^{\eta}|\bar{\psi}_k(\eta)\rangle\Big/\sum_{k=1}^{M}\langle\bar{\psi}_k|\bar{\psi}_k\rangle\ .$$

The structure factor $S^{\eta\eta}(q,\omega)$ is a Fourier transform of the correlation function:

$$S^{\eta\eta}(q,\omega)=\sum_{r}\sum_{t}S^{\eta\eta}(r,t)e^{i(qr-\omega t)}\ , \tag{3.8}$$

where q is the wave vector measured in units of $a=1$, with a being the lattice constant and, hence, $0\le q<2\pi$. We note that, since

$$S^{\eta\eta}(2\pi-q,\omega)=S^{\eta\eta}(q,\omega)$$

holds in the periodic lattice, only $S^{\eta\eta}(q,\omega)$ for $0\le q\le\pi$ will need to be presented in later sections.

Computer CPU time and memory size needed to obtain the correlation functions are roughly estimated to be of order $(M)(2^N)(\text{time}/\tau)$ and $\text{const}\times2^N$, respectively. These are much less than those of a diagonalization technique used conventionally, which are of order $(2^N)^3$ and $(2^N)^2$, respectively. We note that, in principle, the number of states "M" should be sufficiently large, but, as seen later, we can obtain reliable results using only several states ($M\sim5$). Using this method, we can treat systems larger than those treatable by using the diagonalization

technique. In the following sections, we apply the method to obtain the correlation function $S^{zz}(r,t)$ and the structure factor $S^{zz}(q,\omega)$.

IV. RESULTS

We treat the model of $\epsilon=0.1$ on the 1D chain with a periodic boundary condition. The number of spins treated in this paper is up to $N=15$. We choose the number of states $M=4$ or 5 and time interval $J\tau=0.2$.

A. Correlation function $S^{zz}(r,t)$

We first present typical results of $S^{zz}(r,t)$ for systems with odd and even N in Figs. 3 and 4, respectively. Here, we only show them for $r=2n$, which are positive at $t=0$, since those for $r=2n+1$ exhibit a time dependence similar to those for $r=2n$ but have opposite signs. The results depend on whether N is even or odd. This is because for the lattice with an odd N, at least one soliton exists, whereas for an even N, the ground state is close to the doubly degenerate Néel states (see Fig. 1). From $S^{zz}(r,t)$, we readily see the following dynamical properties of the model.

(i) $S^{zz}(r,t)$ slowly oscillates in time and its wave is not simple. This shows that several modes with their frequencies $\omega/J\sim 0$ occur. Their periods are roughly estimated to be longer than $Jt\sim 20$. That is the frequencies are estimated to be $|\omega_{\max}|<0.3J$. This is consistent with the Villain's result, i.e., $|\omega|<4\epsilon J$ with $\epsilon=0.1$.

(ii) The solitons exhibit a propagating nature. This is seen in the time delay of the appearance of the imaginary part of $S^{zz}(r,t)$. Using $Jt\sim 15$ for $r\sim 6$, we estimate the velocity of solitons to be $v\sim 0.4J$. The velocity may also be estimated from a behavior of an individual correlation function $S^{zz}(r,t)$. The sign of $S_0^z(0)S_r^z(t)$ changes whenever one soliton passes the position r. Then, $S^{zz}(r,t)$ for odd N changes its sign as the time goes on. This change in sign occurs in a time interval $Jt\sim 40$ for $N=15$, which leads to $v\sim 0.4J$. The two estimations are consistent with each other and also consistent with the Villain's estimation $v=4J\epsilon\sin(q)$ for $0\le q\le\pi$.

(iii) Besides the slow oscillations, $S^{zz}(r,t)$ exhibits a fast small oscillation, which is seen in the imaginary part of $S^{zz}(r,t)$ in the figures. The period of the oscillation is estimated as $Jt\sim 3$, which leads another peak of $S^{zz}(q,\omega)$ at $\omega/J\sim\pm 2$. The occurrence of the oscillation, or the peak of $S^{zz}(q,\omega)$, was already pointed out by Ishimura and Shiba.[18]

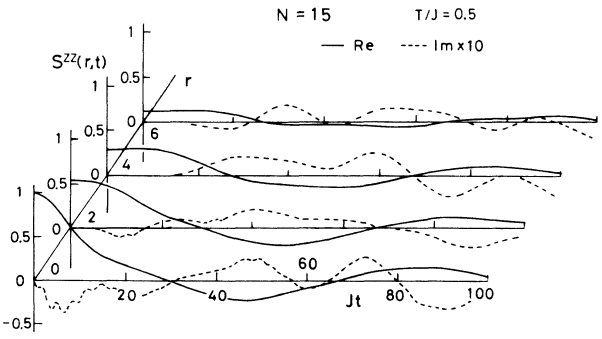

FIG. 3. Correlation functions $S^{zz}(r,t)$ of the model of $\epsilon=0.1$ for odd N. Solid and dashed lines represent real and imaginary parts of them, respectively.

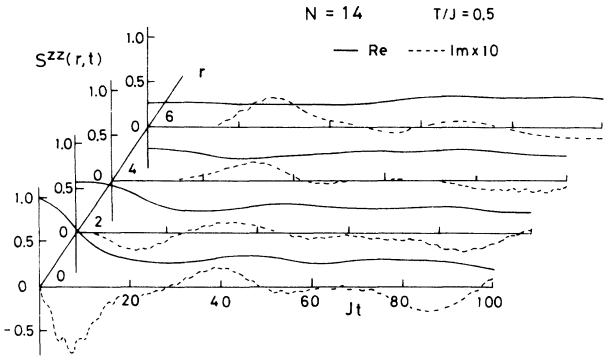

FIG. 4. Correlation functions $S^{zz}(r,t)$ of the model of $\epsilon=0.1$ for even N. Solid and dashed lines represent real and imaginary parts of them, respectively.

All the results support the soliton picture of the spin dynamics of the model. In Sec. IV B we quantitatively analyze the dynamics using the structure factor $S^{zz}(q,\omega)$.

B. Central peak of $S^{zz}(q,\omega)$

The structure factor $S^{zz}(q,\omega)$ is given by Eq. (3.8) in Sec. III. In the calculation, we suppose that the time span in the transformation, which is denoted by "$t_{\max}$" hereafter, is enough to be much longer than N/v, where v is an averaged velocity of solitons. That is $t_{\max}\gg N/v\sim 40/J$, since $v\sim 0.4J$ and $N\sim 15$. To examine this, we made calculations of $S^{zz}(q,\omega)$ using three different $t_{\max}$, i.e., $Jt_{\max}=200$, 400, and 600. The line shapes of $S^{zz}(q,\omega)$ obtained for those three cases do not differ much, except for the difference in resolution of $\Delta\omega$ $(=2\pi/Jt_{\max})$. Hence, we make a calculation of $S^{zz}(q,\omega)$ using data for $Jt=0-400$. The $S^{zz}(q,\omega)$ is real in nature, whereas that obtained in this way is not. Hence, we take the absolute value of it and present it hereafter.

We first consider the peak of $S^{zz}(q,\omega)$ at $\omega\sim 0$. The small peak at $\omega/J\sim\pm 2$ will be considered later. We present results of $S^{zz}(q,\omega)$ at three temperatures $kT/J=0.3$, 0.5, and 0.8. The correlation length r's defined by

$$\langle S_0^z S_r^z\rangle/\langle (S_0^z)^2\rangle=\tfrac{1}{2}$$

for these temperatures are $r\sim 10$, 3, and 1, respectively. At low temperatures, the results for odd and even N differ both in the line shape and in magnitude, whereas they become similar as the temperature increases. Only for odd N and at low temperatures do we find a distinct sharp double peak at $\omega=\pm\Omega(q)$. We discuss those in detail.

In Fig. 5, we present the results for odd N ($N=15$). In this case, $S^{zz}(q,\omega)$ describes the dynamics of odd-soliton states. At low temperatures, only one-soliton states are

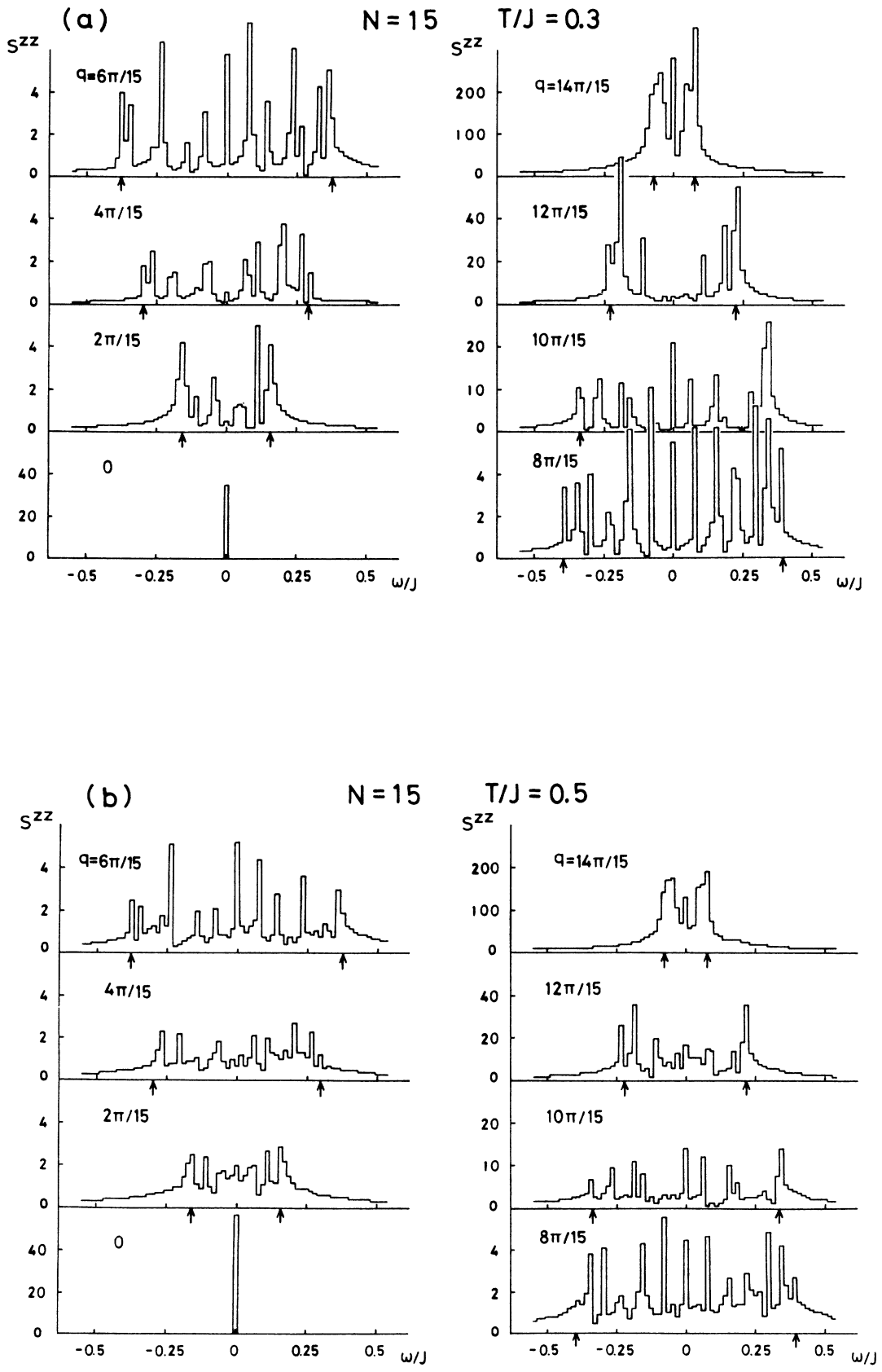

FIG. 5. $S^{zz}(q\omega)$ of the model of $\epsilon=0.1$ for $N=15$ described in an arbitrary unit at various temperatures. Arrows indicate the cutoff frequencies $\pm\Omega(q)$.

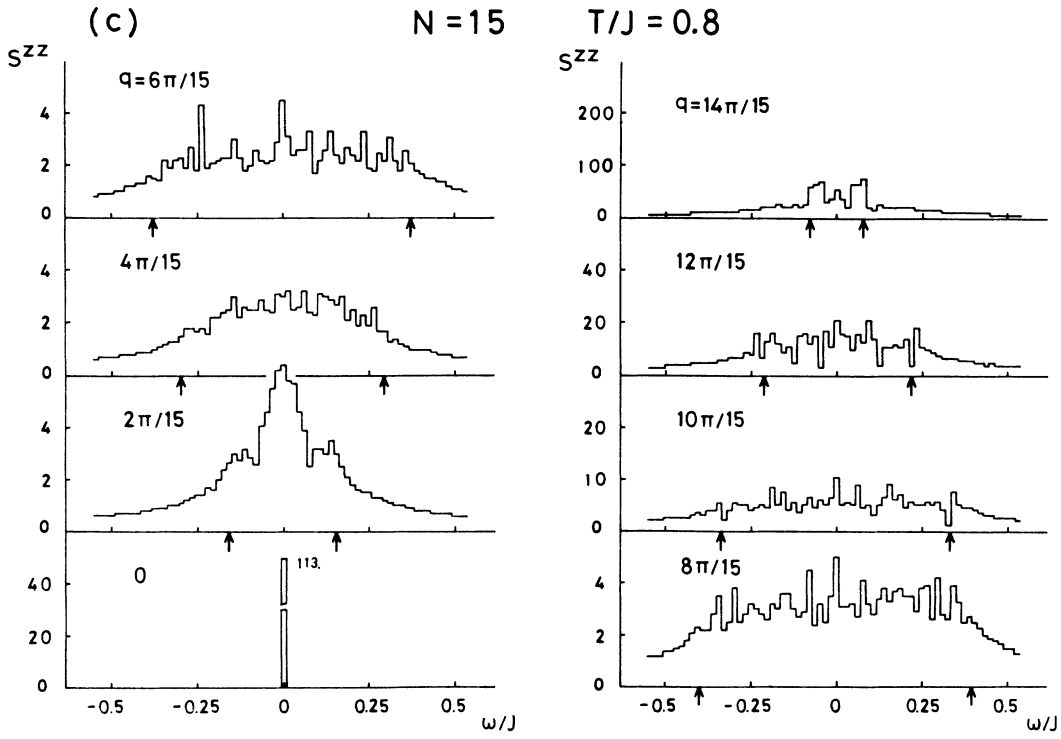

FIG. 5. (*Continued*).

realized and $S^{zz}(q,\omega)$ is described by the states. Although $S^{zz}(q,\omega)$ consists of several spikelike peaks due to the finiteness of the system, it clearly predicts the occurrence of a sharp double peak at $\omega=\pm\Omega(q)$ in a larger system. As the temperature increases, the height of the peak becomes lower and a continuous scattering arises. This is readily recognized, if we remember that $S^{zz}(q,\omega)$ is formally expressed as

$$S^{zz}(q,\omega)=\frac{1}{Z}\sum_{\mu}\sum_{\nu}|\langle\mu|S_q^z|\nu\rangle|^2 e^{-\beta E_\nu}\delta(\omega-E_\mu+E_\nu)$$
$$\sim\frac{\sum\sum_{1s}|\langle\mu|S_q^z|\nu\rangle|^2\delta(\omega-E_\mu+E_\nu)+e^{-2\beta J}\sum\sum_{3s}|\langle\mu|S_q^z|\nu\rangle|^2\delta(\omega-E_\mu+E_\nu)+\cdots}{\sum_{1s}+e^{-2J\beta}\sum_{3s}+\cdots}, \tag{4.1}$$

where $|\mu\rangle$ and $|\nu\rangle$ are eigenstates (soliton states) of the model,

$$S_q^z=(1/\sqrt{N})\sum_r S_r^z\exp(iqr),$$

and $1s$ and $3s$ mean the summations over one- and three-soliton states, respectively. Here, since $\epsilon\ll 1$, we use $E_\nu\sim E_g+J$ for one-soliton states and $E_\nu\sim E_g+3J$ for three-soliton states, respectively, where E_g is the ground-state energy. The number of the one-soliton states is of order N, and that of the three-soliton states is of the order of the combination ${}_NC_3$. As the temperature increases, the relative contribution of the one-soliton states to $S^{zz}(q,\omega)$ decreases, whereas that of three-soliton states increases, being expected to dominate the former. This occurs when ${}_NC_3e^{-2\beta J}\sim N$, which gives $T/J\sim 0.5$ for $N=15$, and a change in the line shape is seen around this temperature. As the temperature increases more, states with more solitons are also excited and $S^{zz}(q,\omega)$ becomes almost flat for $|\omega|<\Omega(q)$.

We note that a similar argument is also possible when N is changed. Since the number of n-soliton states is of order ${}_NC_n$, the number of multisoliton states increases much more rapidly than that of one-soliton states as N increases. In a larger system, the contribution of multisoliton states dominates that of one-soliton states even at low temperatures.

Results for even N ($N=14$) are presented in Fig. 6. For even N, the ground state is the doubly degenerate nonsoliton state and excited states are ones with even number of solitons. In this case, $S^{zz}(q,\omega)$ may be expressed as

$$S^{zz}(q,\omega)\sim 2\delta(\omega)\delta(q-\pi)/\left[2+e^{-2J\beta}\sum_{2s}\cdots\right]$$
$$+\frac{e^{-2\beta J}\sum\sum_{2s}|\langle\mu|S_q^z|\nu\rangle|^2\delta(\omega-E_\mu+E_\nu)+e^{-4\beta J}\sum\sum_{4s}|\langle\mu|S_q^z|\nu\rangle|^2\delta(\omega-E_\mu+E_\nu)+\cdots}{2+e^{-2J\beta}\sum_{2s}+\cdots}. \tag{4.2}$$

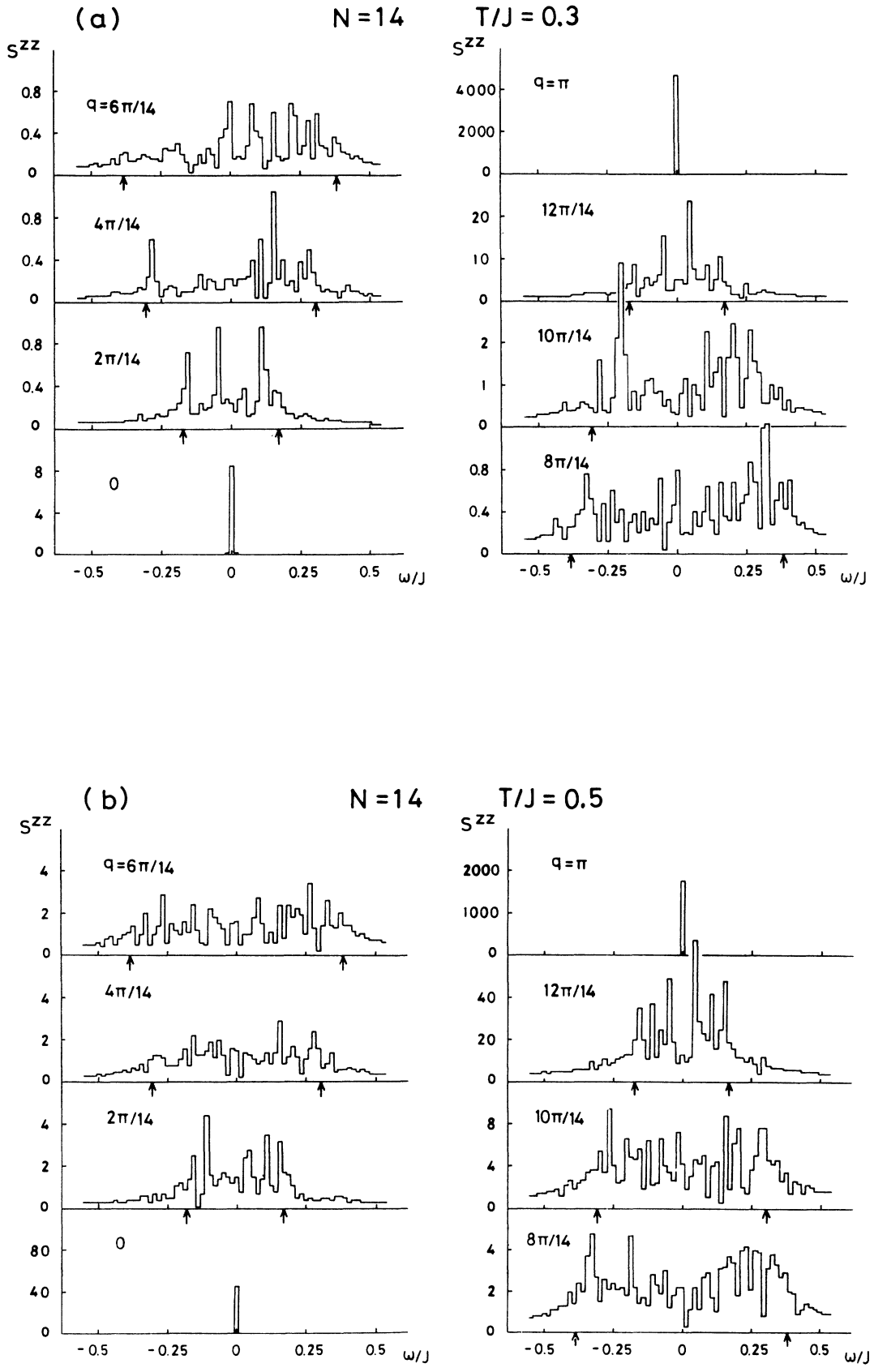

FIG. 6. $S^{zz}(q,\omega)$ of the model of $\epsilon=0.1$ for $N=14$ described in arbitrary units at various temperatures. Arrows indicate the cutoff frequencies $\pm\Omega(q)$.

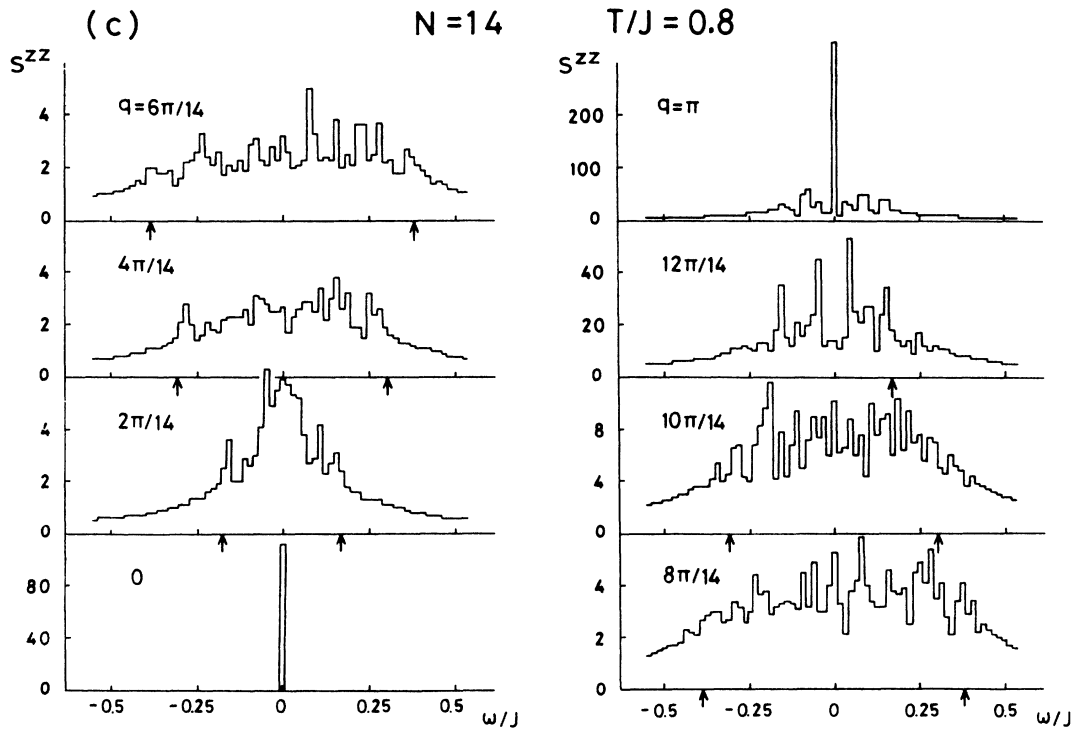

FIG. 6. (*Continued*).

The first term in the right-hand side describes the Bragg-like scattering and the second term the scattering of solitons. As expected, the Bragg-like peak at $q=\pi$ and $\omega=0$ reduces as temperature increases. At low temperatures, the main contribution to $S^{zz}(q,\omega)$ for $q\neq\pi$ comes from two-soliton states. Since the two-soliton term in the numerator has the factor of $e^{-2\beta J}$, $S^{zz}(q,\omega)$ will be very sensitive to temperature. In fact, at $T/J=0.3$, $S^{zz}(q,\omega)$ is much smaller than that for $n=15$, and it becomes of the same order as the temperature increases. At low temperatures, $S^{zz}(q,\omega)$ exhibits only a weak trace of the double peak. As the temperature increases, four-soliton states are also excited and $S^{zz}(q,\omega)$ is described by both two- and four-soliton states. Since $N=14$, the two parts become comparable at $T/J\sim 0.5$ and the line shape of $S^{zz}(q,\omega)$ changes around this temperature. At high temperatures, we get the line shapes similar to those for odd N except for $q\sim\pi$, where the Bragg-like scattering occurs.

C. $S^{zz}(q,\omega)$ at $\omega/J\sim 2$

As mentioned before, $S^{zz}(q,\omega)$ should also have finite values at $\omega/J\sim\pm 2$. The mechanism responsible for the appearance of $S^{zz}(q,\omega)$ at $\omega/J\sim\pm 2$ is different from that at $\omega\sim 0$. In this range of ω, $S^{zz}(q,\omega)$ is described by different soliton states. At low temperatures, those for odd and even N are described by

$$S^{zz}(q,\omega)\sim\frac{\sum_{1s}\sum_{3s}|\langle\mu|S_q^z|\nu\rangle|^2\delta(\omega-E_\mu+E_\nu)+\cdots}{\sum_{1s}+e^{-2J\beta}\sum_{3s}+\cdots}$$

for odd N , (4.3)

$$S^{zz}(q,\omega)\sim\frac{2\sum_{2s}|\langle\mu|S_q^z|\Psi_g\rangle|^2\delta(\omega-E_\mu+E_g)+\cdots}{2+e^{-2\beta J}\sum_{2s}+\cdots}$$

for even N , (4.4)

where $|\Psi_g\rangle$ is one of the ground states approximately described by

$$|\Psi_g\rangle\sim|\Psi_{\text{Néel}}\rangle+\sum_{2s}|\mu\rangle\langle\mu|H_{xy}|\Psi_{\text{Néel}}\rangle/2J\ , \quad (4.5)$$

where $|\Psi_{\text{Néel}}$ is one of the Néel states. Results for $N=15$ and 14 at $\omega/J\sim 2$ are presented in Figs. 7 and 8. The line shapes are different from those for $\omega/J\sim 0$. Only for even N and at low temperatures, can we see a distinct structure of $S^{zz}(q,\omega)$. As the temperature increases, it becomes smaller and disappears. This is because, in both Eqs. (4.3) and (4.4), the denominators increase with the temperature. In contrast to that for $\omega/J\sim 0$, $S^{zz}(q,\omega)$ appears in wide frequency ranges for $q\sim 0$ and π and in narrow ones for $q\sim\pi/2$. This is consistent with that predicted by Ishimura and Shiba.[18] The line shape of $S^{zz}(q,\omega)$, however, is asymmetric with respect to ω, in contrast with their prediction.

V. DIAGONALIZATION IN SUBSPACES

To support the arguments given in Sec. IV, we also calculate $S^{zz}(q,\omega)$ by an alternative method, i.e., a diagonalization technique. Although this method gives the exact result, it is costly in CPU time and memory. Here, since $\epsilon\ll 1$, we calculate it in subspace consisting of low-lying Ising states. For odd N, we take all Ising states with one

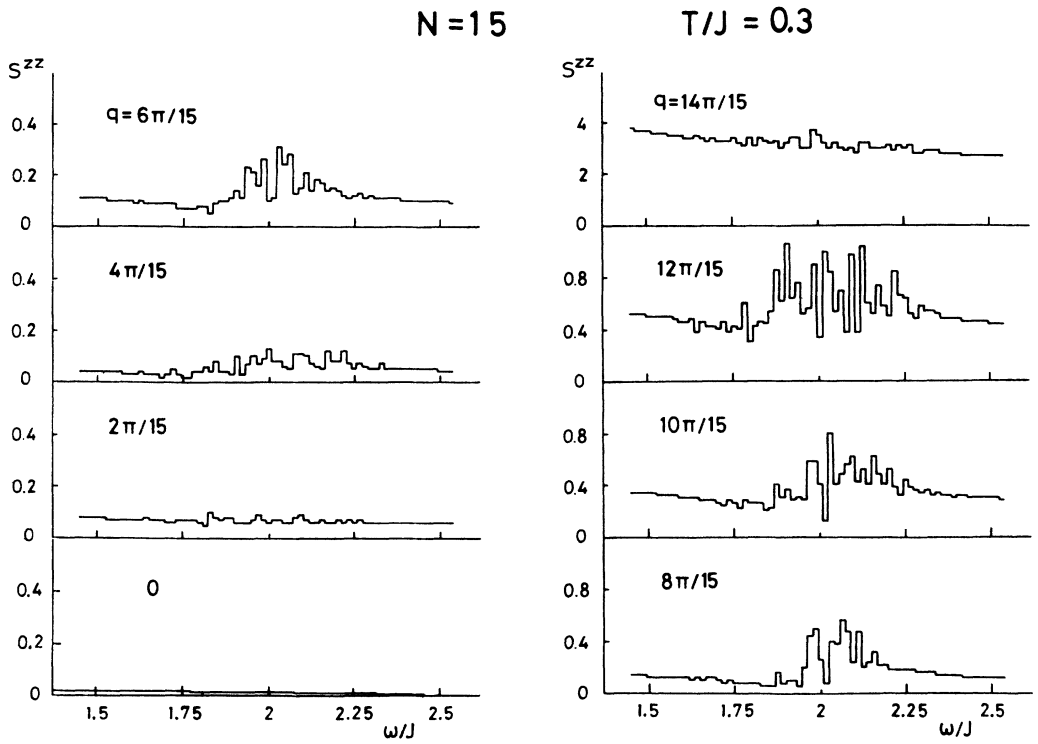

FIG. 7. Side peak of $S^{zz}(q,\omega)$ of the model of $\epsilon=0.1$ for $N=15$ at a low temperature described in arbitrary units.

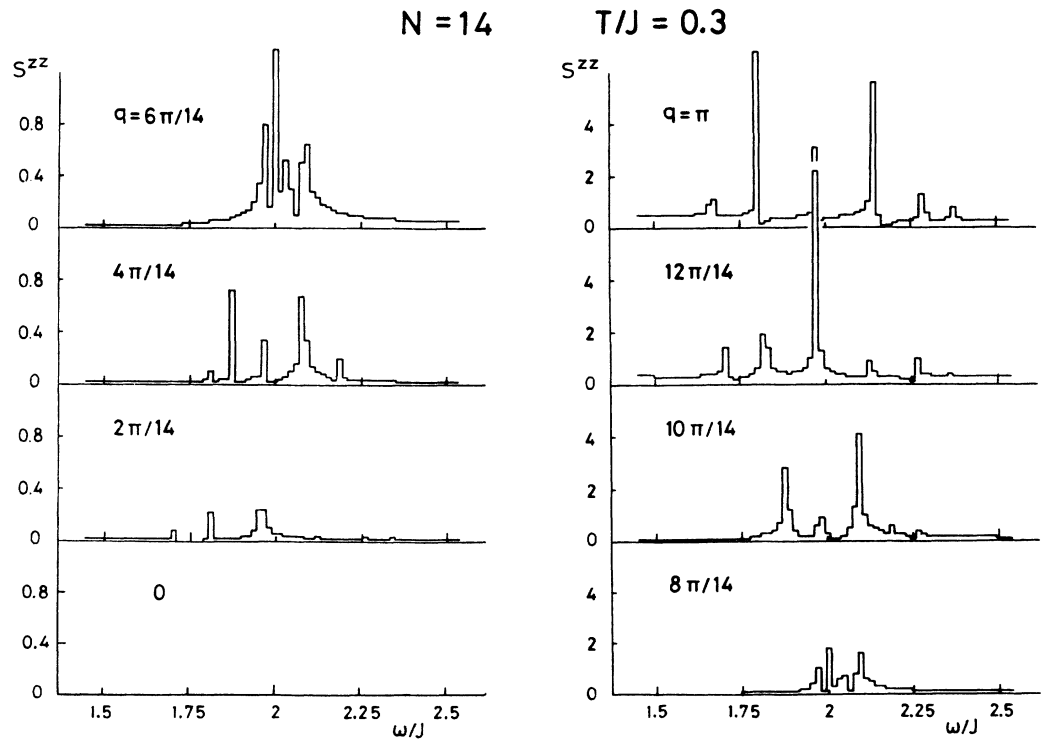

FIG. 8. Side peak of $S^{zz}(q,\omega)$ of the model of $\epsilon=0.1$ for $N=14$ at a low temperature described in arbitrary units.

or three domain walls. For even N, we take the two Néel states and all Ising states with two or four domain walls. Eigenstates obtained in this way, of course, consist of Ising states with different numbers of domain walls. However, we can readily classify them into different soliton states according to the number of domain walls included in the main Ising states. For odd N, $2N$ eigenstates with lower energies are one-soliton states and the others are three-soliton states. For even N, we obtain two- and four-soliton states in addition to two nonsoliton states. We denote the structure factor calculated by using a set of n-soliton states as $S_n^{zz}(q,\omega)$ for distinguishing it from $S^{zz}(q,\omega)$. That is expressed as

$$S_n^{zz}(q,\omega)=\frac{1}{Z_n}\sum_{\mu\nu}|\langle\mu|S_q^z|\nu\rangle|^2 e^{-\beta E_\nu}\delta(\omega-E_\mu+E_\nu)\ , \tag{5.1}$$

where $Z_n=\sum_\nu \exp(-\beta E_\nu)$, and μ and ν run over all n-soliton states. The contribution of n-soliton states to $S^{zz}(q,\omega)$, which is described by $\tilde{S}_n^{zz}(q,\omega)$ hereafter, is straightforwardly obtained from the relation

$$\tilde{S}_n^{zz}(q,\omega)=(Z_n/Z)S_n^{zz}(q,\omega)$$

with Z being the partition function calculated by using all eigenvalues.

A. $\tilde{S}_n^{zz}(q,\omega)$ of each of the soliton states

We first consider the individual $\tilde{S}_n^{zz}(q,\omega)$ and their contribution to $S^{zz}(q,\omega)$. We present the typical results of $S_n^{zz}(q,\omega)$ in Fig. 9 for odd N, in Fig. 10 for even N, and in Fig. 11 for different odd N. The line shapes for different n's are not similar with each other. For $S_1^{zz}(q,\omega)$, a distinct double peak is seen for all q. For $S_2^{zz}(q,\omega)$, although the double peak is seen for $q\sim\pi/2$, it is not so sharp as that found for $S_1^{zz}(q,\omega)$. The larger the number of solitons, the broader the line shape that follows. Results in Figs. 9 and 11 reveal that the contribution of one-soliton states to $S^{zz}(q,\omega)$ decreases as N increases. These line shapes of $S_n^{zz}(q,\omega)$ do not change much when the temperature is varied, because $e^{-\beta E_\nu}\sim e^{-2n\beta J}$ for all n-soliton states for $T/J>4\epsilon$. But, their relative intensities markedly change. This leads to the temperature dependence of the line shape of $S^{zz}(q,\omega)$. As seen in the figures, at temperatures above $T/J=0.5$, three- and four-soliton states contribute considerably to $S^{zz}(q,\omega)$ even for $N\sim 15$. All these results are what we have discussed in Sec. IV.

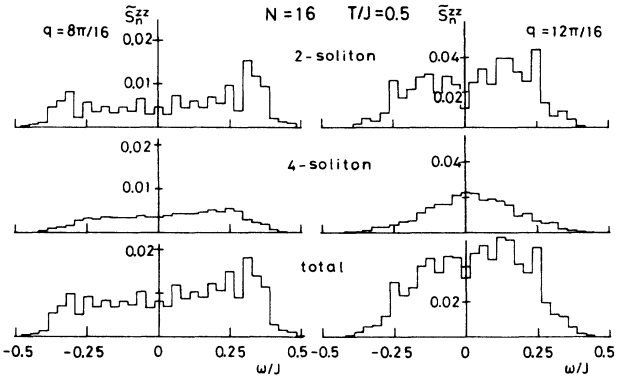

FIG. 10. Contributions of two- and four-soliton states to $S^{zz}(q,\omega)$ for even N (=16) calculated in a subspace described in the text.

It is worthwhile to note that, at low temperatures, $S^{zz}(q,\omega)$ obtained here are very similar to those presented in Sec. IV, although both are obtained based on different approximations. This proves the reliability of both the methods used in this paper.

B. Extrapolation to a larger N

Since a large number of solitons are thermally excited in a larger system, the line shape is not the same as predicted by previous theories in which only one- and two-soliton states are treated. Which line shape is obtained for $N\to\infty$? To answer this question, it is necessary to treat much larger systems of $N\gg r$, where r is the correlation length of the model. For $T/J>0.5$, since $r\lesssim 3$,

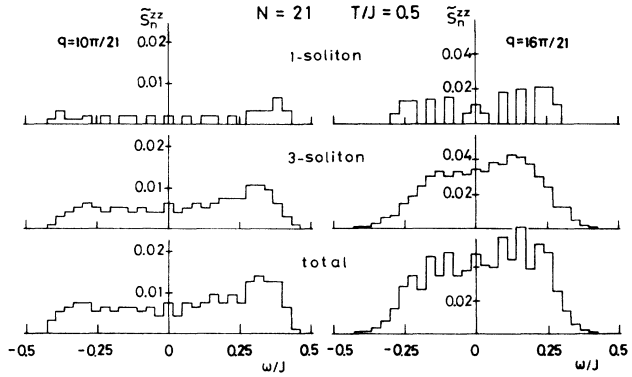

FIG. 9. Contributions of one- and three-soliton states to $S^{zz}(q,\omega)$ for odd N (=21) calculated in a subspace described in the text.

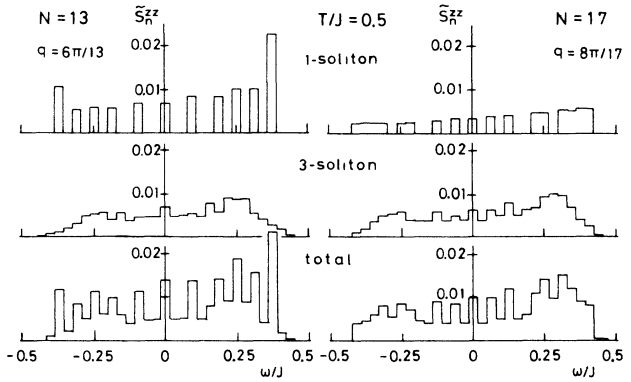

FIG. 11. Contributions of one- and three-soliton states to $S^{zz}(q,\omega)$ for different odd N calculated in a subspace described in the text.

the systems treated in this paper ($N \lesssim 15$) are not small and, in fact, give results almost independent of N. At lower temperatures, since r rapidly increases with decreasing temperature, it is difficult to obtain $S^{zz}(q,\omega)$ in the same manner.

For a larger N, $S^{zz}(q,\omega)$ will be approximately described by the n-soliton states with $n \sim \rho N$, i.e., $S^{zz}_{\rho N}(q,\omega)$, where $\rho \sim 1/(2r)$ is the density of solitons. In Figs. 12 and 13, we show $S^{zz}_{\rho N}(q,\omega)$ for different N for two densities of ρ $(=n/N) \sim \frac{1}{7}$ and $\frac{1}{4}$. In fact, those converge rapidly as N increases. This fact may be used to estimate $S^{zz}(q,\omega)$ in a larger system. A procedure for the estimation of the line shape at a given temperature T_0 is as follows. We first estimate the density ρ at T_0 using the relation $\rho \sim 1/(2r)$, with r being determined by $\langle S^z_0 S^z_r \rangle / \langle (S^z_0)^2 \rangle = \frac{1}{2}$. Then $S^{zz}_{\rho N}(q,\omega)$ is calculated with increasing N like those discussed earlier. When the function converges, we regard it as $S^{zz}(q,\omega)$ at T_0. Since $\rho \sim \frac{1}{7}$ and $\frac{1}{4}$ are realized at $T/J \sim 0.4$ and 0.55, we may regard $S^{zz}_n(q,\omega)$ shown in Figs. 12 (and also in Fig. 9) and 13 as $S^{zz}(q,\omega)$ at those temperatures, respectively. Note that, as pointed out before, the line shapes of individual $S^{zz}_n(q,\omega)$ do not depend much on the temperature.

At much lower temperatures, the method also becomes useless to estimate $S^{zz}(q,\omega)$, because we need to treat much larger systems. For example, at $T/J \sim 0.3$, we need at least to calculate $S^{zz}_3(q,\omega)$ of a system with $N \sim 50$. However, we can guess the line shape from the results presented here. In particular, the results in Figs. 12 and 13 are suggestive. For a fixed density ρ, the peaks become broader as N increases. We also see that the line shape does not change qualitatively when the density is lowered from $\rho \sim \frac{1}{4}$ to $\frac{1}{7}$, although the peak positions move to the higher frequency side. We believe, hence,

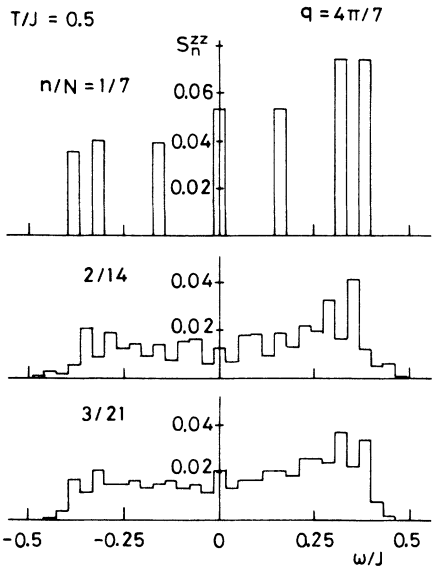

FIG. 12. $S^{zz}_n(q,\omega)$ at a fixed soliton density of ρ $(=n/N)=\frac{1}{7}$. Note those for $N \to \infty$ are regarded as $S^{zz}(q,\omega)$ at $T/J \sim 0.4$.

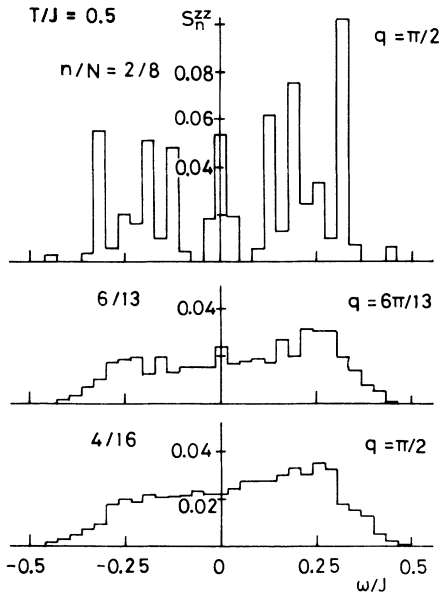

FIG. 13. $S^{zz}_n(q,\omega)$ at a fixed soliton density of ρ $(=n/N)=\frac{1}{4}$. Note those for $N \to \infty$ are regarded as $S^{zz}(q,\omega)$ at $T/J \sim 0.55$.

that $S^{zz}(q,\omega)$ exhibits a broad double maximum at all temperatures below a certain temperature, above which the soliton picture breaks down.

VI. COMPARISON WITH EXPERIMENTS ON $CsCoBr_3$ AND $CsCoCl_3$

Now we make a comparison between our results and the experimental observations of the central peak. First we consider $CsCoBr_3$, for which $\epsilon = 0.10$ or 0.14 (Refs. 14 and 15) is estimated, together with $J = 77.8$ K. Using the values of $J = 78$ K and $\epsilon = 0.1$ and the method in Sec. III, we calculate $S^{zz}(q,\omega)$. Our results reproduce the line shape very well. However, the frequency range of the peak is about 1.8 times as narrow as compared with experimental observations. We think this difference comes from the difference between the values of ϵ. So long as $\epsilon \ll 1$, the line shape will depend little on the value of ϵ, except the frequency range increases in proportion to ϵ. Assuming $\epsilon = 0.18$, we expand the frequency range 1.8 times and plot the results in Figs. 14 and 15 for different wave vectors and temperatures, together with experimental observations by Nagler *et al.* (Figs. 17 and 18 in Ref. 15). Since in our calculation $S^{zz}(q,\omega)$ has a background associated with the finiteness of time span $t_{\max}$, we subtract the background so as to fit our results and the experimental results at higher frequencies. Then, the ordinate scale is chosen so that our result for $q = 8\pi/14$ at $T = 0.65J$ (~ 51 K) fits the experimental result for $q = (1.2, 0, 0.5)$ at $T = 50$ K [Fig. 17(b) in Ref. 15]. This scaling factor is commonly used in all histograms in Figs. 14 and 15. Note, since we can only take distinct values of q because of the finiteness of the system, we choose the nearest value of q, which is shown in brackets in the figures.

Considering the fact that the scaling factor and ϵ ($=0.18$) are the only adjustable parameters used in this comparison, the agreement is quite remarkable both in the line shape and in the temperature dependence. Note, our estimation of ϵ is a little greater than that estimated from an analysis of a dispersion of central modes based on the Villain's theory, in which the peak position is given by the cutoff frequency $\omega=\Omega(q)$.[15] The discrepancy comes from the fact that the peak of $S^{zz}(q,\epsilon)$ does not occur at $\Omega(q)$ but inside $\Omega(q)$. Hence, we believe the present estimation is more plausible.

Next, we consider experimental observations on $CsCoCl_3$ by Yoshizawa *et al.* (Fig. 5 in Ref. 13) in which $\epsilon=0.14$ and $J=74$ K are estimated.[13] Our results for $\epsilon=0.1$ reproduce the line shape very well except for the frequency range. Assuming $\epsilon=0.15$ and following a similar method given earlier for the scaling, we plot our results in Fig. 16, together with the experimental results. Here we also take into account the small deviations of q between the experiment and the calculation, which lead to differences in Villain's cutoff frequency $\Omega(q)$. We again see a very good agreement between the experimental and calculated results. Experimentally observations on the same substance at low temperatures ($T\leq 30$ K) were made by Boucher *et al.*[16] for $q\lesssim\pi$. It is difficult to make a similar comparison at the temperatures, because our simulation results depend on the number of spins. By

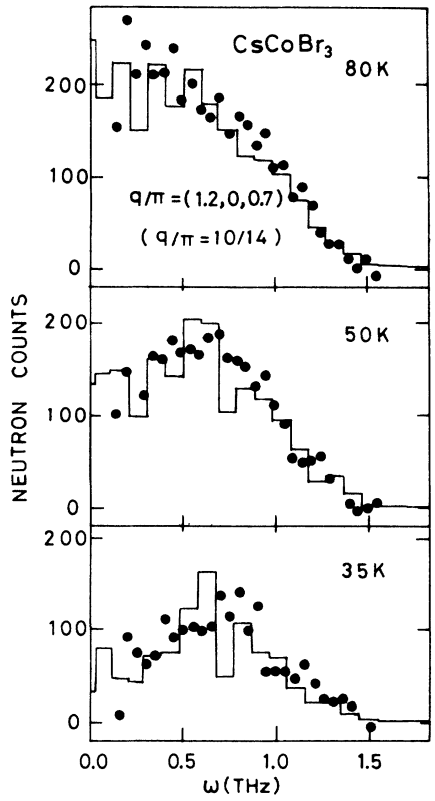

FIG. 15. Comparison between our results (histogram) obtained for $J=78$ K and $\epsilon=0.18$ and experimental results on $CsCoBr_3$ by Naglar *et al.* (Fig. 18 in Ref. 15).

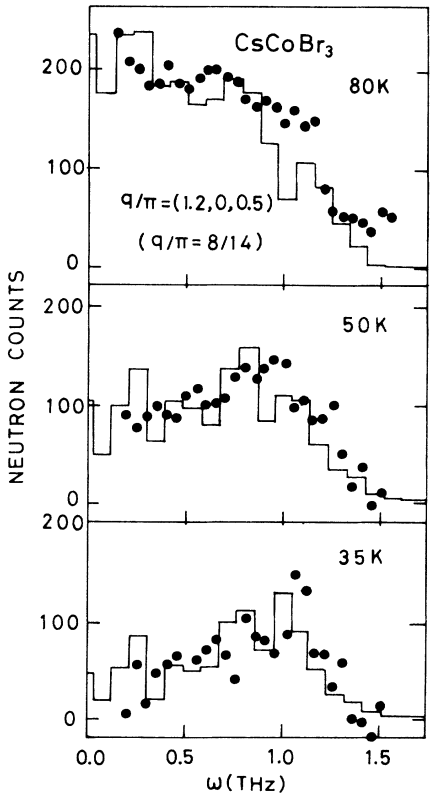

FIG. 14. Comparison between our results (histogram) obtained for $J=78$ K and $\epsilon=0.18$ and experimental results on $CsCoBr_3$ by Naglar *et al.* (Fig. 17 in Ref. 15).

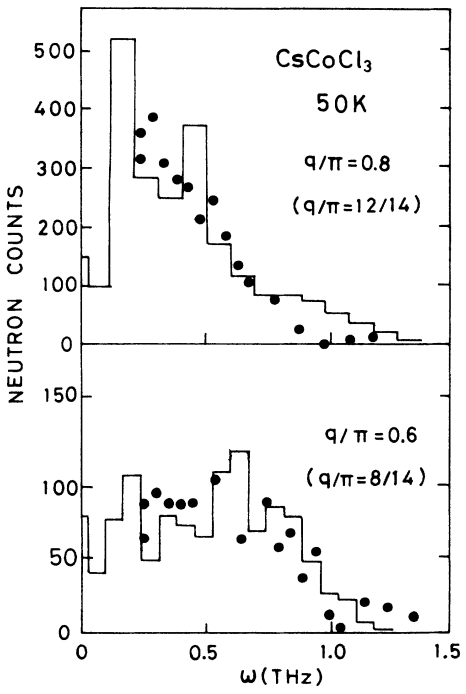

FIG. 16. Comparison between our results (histogram) obtained for $J=74$ K and $\epsilon=0.15$ and experimental results on $CsCoCl_3$ by Yoshizawa *et al.* (Fig. 15 in Ref. 13).

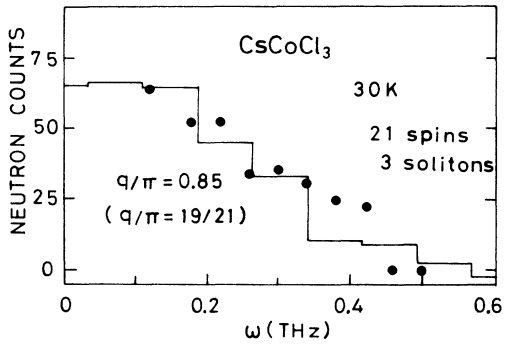

FIG. 17. Comparison between our results (histogram) obtained for $J=74$ K and $\epsilon=0.15$ and experimental results on $CsCoCl_3$ by Boucher *et al.* (Fig. 7 in Ref. 16).

using the extrapolation method given in Sec. V, however, $S^{zz}(q,\omega)$ at the highest temperature $T=30$ K can be estimated. Since $T/J\sim 0.4$ for $T=30$ K, then the line shape of $S_3^{zz}(q,\omega)$ for $N=21$ is compared with the experimental one, which is shown in Fig. 17. A good agreement is also seen. The comparison at lower temperatures is difficult to do at present. We note, however, that experimental results for $q \lesssim \pi$, reveal the occurrence of a shoulder and a gradual decrease outside the $\omega=\Omega(q)$. These are consistent with those suggested in Sec. V.

VII. CONCLUSIONS

A simulation of solitons in an Ising-like antiferromagnet on a finite 1D lattice with N spins has been made. Space-time correlation functions $S^{zz}(r,t)$ and their Fourier transforms, i.e., the dynamical structure factors $S^{zz}(q,\omega)$, have been obtained for different N at various temperatures. A slow but large oscillation of $S^{zz}(r,t)$ has been seen, which gives a direct evidence of the occurrence of propagating domain walls, i.e., solitons. The oscillation leads to a low-energy component of $S^{zz}(q,\omega)$ whose line shape depends a great deal on whether N is even or odd and on temperature. Only for odd N and at low temperatures, a sharp double peak of $S^{zz}(q,\omega)$ is seen at cutoff energies $\pm\Omega(q)$ predicted by previous theories. As temperature increases, the peak becomes very broad irrespective of N being even or odd. These points have been argued in detail by using a soliton picture of the Ising-like model.

To support the argument, we have analyzed the model in a subspace consisting of low-lying Ising states using a diagonalization technique. Eigenstates are classified into different soliton states. We have shown that different soliton states give their own line shapes of $S^{zz}(q,\omega)$, i.e., the larger the number of solitons, the broader the peak. As temperature increases or N becomes larger, the line shape becomes broader, because the number of thermally excited solitons increases. From the results, we have concluded that, in an infinitely large system, the line shape is broad at all temperatures in contrast with that predicted by previous theories.

Comparisons between our results and experimental results on $CsCoBr_3$ and $CsCoCl_3$ have been made. Very good agreements are obtained in both the line shape and the temperature dependence. We conclude that the spin dynamics of the substances are well described by the Ising-like model on the purely 1D chain. Other interactions such as interchain interactions need not be taken into account to explain the dynamics of the substances.

Finally, we should mention that the dependence of soliton number on the line shape of $S^{zz}(q,\omega)$ is dramatic. The larger the number of solitons, the broader the line shape becomes. We believe that the broadening comes from an inherent nature of solitons in this model. That is when two solitons collide with each other, they are rebounded like two hard rods. Then, each soliton moves in a space between two neighboring solitons. Of course, the size of the space distributes around an averaged value of order $2r$, with r being the correlation length of the model. Moreover, the two neighboring solitons also move in time being governed by the same dynamics. These will contribute to the broadening of the line shape. This will be discussed separately. In this paper, we have studied the longitudinal response function $S^{zz}(q,\omega)$. Our method is also applicable to the analysis of the transverse response function $S^{xx}(q,\omega)$. This will be given in a future paper.

ACKNOWLEDGMENTS

The authors would like to thank Mr. H. Ohhara for helping with the numerical calculations.

[1]H. J. Mikeska, J. Phys. C **11**, L29 (1978).
[2]T. Tsuzuki and K. Sasaki, Prog. Theor. Phys. Suppl. No. **94**, 73 (1988), and references therein.
[3]J. K. Kjems and M. Steiner, Phys. Rev. Lett. **41**, 1137 (1978).
[4]L. P. Regnault, J. P. Boucher, J. Rossat-Mignod, J. P. Renard, J. Bouillot, and W. G. Stirling, J. Phys. C **15**, 1261 (1982).
[5]See references cited in Ref. 2.
[6]M. D. Johnson and N. F. Wright, Phys. Rev. B **32**, 5798 (1985).
[7]H. Benner, J. Wiese, R. Geick, and H. Sauer, Europhys. Lett. **3**, 1135 (1987).
[8]J. Villain, Physica **79B**, 1 (1975).
[9]H. Shiba, Prog. Theor. Phys. **64**, 466 (1980); W. P. Lehmann, W. Breitling, and R. Weber, J. Phys. C **14**, 4655 (1981).
[10]K. Adachi, M. Hamashima, Y. Ajiro, and M. Mekata, J. Phys. Soc. Jpn. **47**, 780 (1979).
[11]K. Adachi, J. Phys. Soc. Jpn. **50**, 3904 (1981).
[12]J. P. Boucher, G. Rius, and Y. Henry, Europhys. Lett. **4**, 1073 (1987).
[13]H. Yoshizawa, K. Hirakawa, S. K. Satija, and G. Shirane, Phys. Rev. B **23**, 2298 (1981).
[14]S. E. Nagler, W. J. L. Buyers, R. L. Armstrong, and B. Briat, Phys. Rev. Lett. **49**, 590 (1982); S. E. Nagler, W. J. L. Buyers, R. L. Armstrong, and B. Briat, Phys. Rev. B **27**, 1784 (1983).
[15]S. E. Nagler, W. J. L. Buyers, R. L. Armstrong, and B. Briat, Phys. Rev. B **28**, 3873 (1983).
[16]J. P. Boucher, L. P. Regnault, J. Rossat-Mignod, Y. Henry, J.

Bouillot, and W. G. Stirling, Phys. Rev. B **31**, 3015 (1985).
[17]W. J. L. Buyers, M. J. Hogan, R. L. Armstrong, and B. Briat, Phys. Rev. B **33**, 1727 (1986).
[18]N. Ishimura and H. Shiba, Prog. Theor. Phys. **63**, 743 (1980).
[19]M. Imada and M. Takahashi, J. Phys. Soc. Jpn. **55**, 3354 (1986).
[20]F. Matsubara and S. Inawashiro, Solid State Commun. **67**, 229 (1988).